==========

Figures, tables, and some mathematical expressions are available in GIF format in this directory. These files have the naming convention FIGn.GIF, TABn.GIF or EQNn.GIF. Images taken from the paper should be considered parts of the paper, and all copyrights must be respected.

==========

Pioneer Venus Orbiter Planar Retarding Potential Analyzer Plasma Experiment

WILLIAM C. KNUDSEN, KARL SPENNER, JACK BAKKE, AND VIT NOVAK

***Abstract*-The retarding potential analyzer (RPA) on the Pioneer Venus Orbiter Mission measures most of the thermal plasma parameters within and near the Venusian ionosphere. Parameters include total ion concentration, concentrations of the more abundant ions, ion temperatures, ion drift velocity, electron temperature, and low-energy (0-50 eV) electron distribution function. Several functions not previously used in RPA's were developed and incorporated into this instrument to accomplish these measurements on a spinning spacecraft with a small bit rate. The more significant functions include automatic electrometer ranging with background current compensation; digital, quadratic retarding potential step generation for the ion and low-energy electron scans; a current sampling interval of 2 ms throughout all scans; digital logic inflection point detection and data selection; and automatic ram direction detection.**

I. Introduction

THE PLANAR retarding potential analyzer (RPA) designed and developed for the Pioneer Venus Orbiter Mission is an instrument of advanced design benefitting from steady progress in planar RPA design over the past approximately twenty years of the space age [1]-[8] .

It measures most of the essential plasma quantities required to define the state and motion of the ionospheric plasma, and also measures the temperature and concentration of the solar wind electrons.

The Pioneer Venus mission is described in some detail elsewhere and will not be repeated here [9], [10] . The RPA repeatedly enters the ionosphere of Venus aboard the spinning orbiter spacecraft, and measures ionospheric plasma quantities as well as plasma quantities of the solar-wind-ionosphere interaction region in the energy range 0-50 eV.

The quantities measured by the orbiter RPA are electron temperature T_e, total ion concentration N_i, individual ion temperature T_i^j, of the most abundant species, their concentrations N_i^j, thermal ion drift velocity $\bar{}$D, and energy distribution of suprathermal electron and ion fluxes f(E) up to 50 eV. Table I summarizes these quantities and gives the expected spatial resolutions, ranges, and uncertainties.

II. Instrument Principles and Characteristics

Fig. 1, a photograph of the assembled RPA, illustrates the sensor surrounded by a 30-cm diameter ground plane. Fig. 2 shows the RPA integrated with the Pioneer Venus orbiter spacecraft. An alignment fixture is covering the sensor grids in this latter photograph. The planar sensor consists of a sequence of grids as shown in Fig. 3. The physical quantities can be derived for a plasma from the integral flux of ions or electrons, gathered by collector C, as a function of energy. Only particles whose energy is greater than the retarding voltage applied on the retarding grid G_2 can strike the collector. Use of appropriate voltage programs allows analysis of the particle energy. The other grids and the collector are biased with control voltages which separate positive and negative particles and minimize secondary electrons produced by particle impact and photons.

The orbiter RPA operates in three principal modes, a thermal electron mode, an ion mode, and a suprathermal electron mode. The control voltages and retarding potential programs for these modes are defined in Tables II and III. The principal modes with different operating options are selected through ground command.

III. Electron Mode

In the electron mode, the ion current to the collector is negligible with the collector at 47 V. A potential difference of 20 V between G_4 and C was found sufficient to suppress most of the secondary electrons produced by ion or electron impact at the collector. The three front grids G_o, G_1, and G: are the energy analyzing grids. They are stepped together from +6.8 to - 4.2 V in the coarse scan. The corresponding collector current is measured by a logarithmic electrometer and then digitized. Fig. 4 illustrates a characteristic curve returned by the RPA while operating in the electron mode with I-V option. The straight-line portion of the characteristic curve in which the logarithm of the current is proportional to the retarding potential is the retarding region, and the shape of the straight line determines the electron temperature by the relation

$$T_e = -\left(\frac{e}{k}\right)\frac{\Delta V}{\Delta \log(-I_e)}$$

where e is the electron charge; k the Boltzmann constant; and I_e the electron current. The left side with larger positive voltage is the attractive region. The voltage V_p at which these two portions of the curve join is the potential of plasma relative to spacecraft. Within the ionosphere, it has been varying from a few tenths volt negative to three volts positive. At the lower end of the retarding region, the current decreases more slowly with an increase in retarding potential than it did in the retarding region because of a population of ambient photoelectrons with high energy. The strong decrease in current at the end of the retarding voltage range results from the presence of a compensating current added by the RPA instrument. At the maximum retarding voltage of each mode, the RPA adds current of the appropriate sign and magnitude to the electrometer input to decrease the absolute value of the total current to less than approximately 2 X 10^{-12} A [8] . This current compensation reduces the influence of high-energy particles and photoelectrons produced within the RPA by solar radiation on the measurement of thermal plasma quantities.

The RPA is usually operated in a "peak option" state in which the retarding region is automatically recognized by the RPA, and either 5 or 11 values of $\Delta \log(-I_e)(=\log^* (I_{eJ}/I_{eJ+1}))$ spaced around the retarding region are selected depending on command option and returned to earth. Onboard logic forms the first and second finite differences of the successively digitized values of log ($-I_e$) When a sequence of these values satisfy a peak criterion, the logic selects 5 or 11 values of $\Delta \log(-I_e)$ about the peak and the retarding potential step number for transmission to earth. Values of $\Delta\log(-I_e)$ selected and returned from Venus by the RPA are illustrated in the lower portion of Fig. 4. The retarding voltage step program in the "peak option" consists of a coarse scan over the entire voltage range followed by one or three fine scans over the appropriate subrange centered where the largest difference in the coarse mode has occurred (Table III). The $\Delta \log(-I_e)$ values measured in the fine scan have been multiplied by four for proper comparison with the values measured in the coarse scan. The retarding voltage at which the largest value of $\Delta \log(-I_e)$ occurs in the coarse electron scan is quite close to the plasma potential and is used as the starting potential (reference potential) for the quadratic ion retarding potential step program.

The purpose for the coarse and fine electron retarding scans is to measure a large range of temperatures. The RPA has operated successfully in the thermal-electron peak mode from 300 to 25 000 K. Temperatures above approximately 25 000 K are measured in the suprathermal electron mode.

IV. Ion Mode

With the collector at - 4.6 V and suppressor grid at - 24.6 V, ambient electrons with energy less than approximately 24.6 eV are not collected. Ions with sufficient kinetic energy to overcome the retarding potential on grid G_2 (Fig. 3) are collected. An ion-characteristic curve measured by the RPA in the Venus ionosphere is illustrated by the dots in Fig. 5. The retarding potential V is related to the step lettered J by the equation

$$V_J - V_{ref} = \frac{J(J-1)}{2} 0.011 \text{ V}$$

where V_{ref} is a voltage close to the plasma potential sensed and established in the electron mode. The current corresponding to every other step value is returned by the RPA when operating in the ion mode with I-V option. The solid line is the least square fit of the appropriate theoretical expression for the total current to the data points [8]. The derived quantities are listed in the figure.

When operating in the "peak option" the RPA forms differences in current $\Delta I_j (= I_j - I_{j+1})$ measured at successive retarding potential steps and returns either 5 alternate or 11 successive values of ΔI_j around sensed peaks in ΔI.

Examples of ΔI values returned around O^+ and O^+_2 peaks are also illustrated in Fig. 5. The same digital peak criterion is used to recognize the ion peaks as is used to recognize the retarding region of the electron characteristic curve. It is shown elsewhere [8] that the ΔI values about a peak are approximately Gaussian in shape. The half-width of the peaks is proportional to the square root of the ion temperature T_i, and the peak value of ΔI_j is proportional to the ion concentration divided by $\sqrt{T_i}$. The value of J at which the peak occurs is proportional to the square root of the ion kinetic energy normal to the RPA grids. The ion temperature, concentration, mass, and velocity normal to the RPA grids are derived by numerically fitting the theoretical expression for ΔI_j to the measured values of ΔI_j with use of the least squares criterion. The solid curve in the lower-half of Fig. 5 is drawn through the theoretical values of ΔI_j. The geophysical quantities derived from the fit are listed. In computing the theoretical values of ΔI_j (and also I_j), an ion of mass 13 was assumed present with a concentration equal to 7 percent of the O+ concentration.

V. Vector Ion-Drift Velocity

Vector ion-drift velocity is measured by measuring three single components of the velocity in three different directions. Fig. 6 illustrates the principle of measurement. From the analysis of data from a single sweep of the RPA, the component of total ion velocity normal to the RPA grids is derived. A single sweep of the RPA requires approximately 0.16 s during which time the spacecraft rotates through 5° about its spin axis. The telemetry bit rate assigned to the RPA permits only one sweep of data to be telemetered to earth per spacecraft spin period. Consequently, to achieve a vector measurement of the ion drift velocity, one sweep of data is recorded in each of three successive spin periods at three different roll angles. With the RPA measurement axis offset from the spin axis by 25° the necessary three independent component measurements are achieved. The first ion sweep designated I_1 is recorded when the total ion velocity relative to the spacecraft lies in or close to the plane defined by the spacecraft spin axis and the RPA sensor axis. Sweep I_2 is recorded in the subsequent spin period 45° in roll angle before that at which I_1 was recorded. Sweep I_3 is recorded in the third spin period at a roll angle 45° greater than that at which I_1 was recorded.

The roll angle at which I_1 is recorded is defined by receipt of a "Ram" signal from the spacecraft or by sweep with largest saturation ion current.

VI. Suprathermal Electron Mode

The collector and guard ring are biased at +47 V in the suprathermal electron mode to collect electrons and the grid G_1 is biased at +47 V to prevent positive ionospheric ions from impinging on the retarding grid G_2 [11]. The retarding grid G_2 is stepped quadratically from 0 to -50 V during which time the electron currents are digitized for telemetering to earth. The RPA may be programmed to record one suprathermal-electron characteristic curve every fifth-spin revolution, the other four revolutions being used to record one thermal-electron sweep followed by three ion sweeps, or it may be programmed to record one suprathermal-electron sweep every spin revolution with successive sweeps spaced 90° in roll angle from each other. In this latter mode of operation, only suprathermal-electron data are recorded.

The electron energy distribution function f_e is derived from the set of electron currents with use of the Druyvesteyn [12] relation:

$$f_e = \frac{V}{e^2\pi}\frac{d^2I}{dV^2}.$$

In regions of space where the electron energy distribution is expected to be Maxwellian, the parameters of the Maxwellian distribution, temperature, and concentration are derived by fitting a straight line to the curve of log I_e versus V.

Fig. 7 shows an example of the suprathermal-electron currents measured in the dayside ionosphere and the derived electron-energy distribution.

VIII. Inflight Calibration

The RPA is commanded periodically into an inflight calibration sequence. In the first part of the sequence, the electrometer is disconnected from the collector and a sequence of internal calibration currents satisfying the peak selection criteria are applied to the electrometer to evaluate the electrometer sensitivity and peak selection logic. In subsequent portions of the calibration sequence, the internal noise of the electrometer in its most sensitive range is measured, and the retarding voltages are sampled to verify amplifier gain and proper logic operation.

VIII. Instrument Parameter Summary

The following table summarizes the more important physical and electrical properties of the RPA.

IX. Conclusions

The Pioneer Venus orbiter RPA is measuring a large number of the plasma quantities needed to define the state and motion of the ionospheric plasma. These measurements are contributing to a detailed definition of the ionosphere and to an understanding of the processes affecting it [13]-[15]. Measurements from the suprathermal-electron mode are contributing to the detailed definition of the ionosheath, ionosphere and mantle plasmas, and the boundaries separating them [16]. The RPA is an instrument of advanced design and has been operating continuously and as designed for approximately fifteen months since launch at the time of preparation of the manuscript (Aug. 1979).

Acknowledgment

We wish to acknowledge the dedicated efforts of many people who contributed to the development of the orbiter RPA. Special mention should be made of Dr. J. Reagan, S. Bjerklie, J. McDaniel, V. Waltz, J. Parker, and K. Fong of the Lockheed Palo Alto Research Laboratory, W. Ott of the Institut fur Physikalische Weltraumforschung, K. Polzer, G. Kupfahl, E. Eichhom, H. Bauer, V. Gerber, K. Sudholt, A. Kronthaler, and E. Spemmann of Messerschmitt-BolkowBlohm GmbH, Mr. Guenther and Dr. Klinkman of DFVLRIBPT, and E. Tischler and A. Wilhelmi of NASA/AMES.

The fnancial support for W. C. Knudsen, J. Bakke, and the Lockheed Palo Alto Research Laboratory for the development of the control electronics subassembly and integration of the instrument on the spacecraft was provided by NASA. The fnancial support for K. Spenner, V. Novak, the Institut fur Physikalisches Weltraumforschung and Messerschmitt-BolkowBlohm GmbH for the development of the sensor subassembly and its electronics was provided by the Bundesminister fur Forschung und Technologie of the Federal Republic of West Gemmany.

References

[1] H. E. Hinteregger, "Combined retarding potential analysis of photoelectrons and environment charged particles up to 234 km," *Space Res.,* vol. 1, pp. 304-327, 1960.

[2] W. B. Hanson and D. D. McKibbin, "An ion trap measurement of the ion concentration profile above the F2 peak," *J. Geophys. Res.,* vol. 66, pp. 1667-1671,1961.

[3] W. C. Knudsen, "Evaluation and demonstration of the use of retarding potential analyzers for measuring several ionospheric quantities," *J. Geophys. Res.*, vol. 71, pp. 4669-4678, 1966.

[4] K. K. Harris, G. W. Sharp, and W. C. Knudsen, "ion temperature and relative ion composition measurements from a low-altitude polar-orbiting satellite," *J. Geophys. Res.,* vol. 72, pp. 5939

[5] W. B. Hanson, S. Sanatani, D. Zuccaro, and T. W. Flowerday "Plasma measurements with the retarding potential analyzer on Ogo 6,"*J. Geophys. Res.,* vol. 75, pp. 5483-5501, 1970.

[6] W. B. Hanson, D. R. Zuccaro, C. R. Lippincott, and S. Sanatani "The retarding potential analyzer on atmosphere explorer," *Radio Sci.,* vol. 8, pp. 333-340, 1973.

[7] K. Spenner and A. Dumbs, "The retarding potential analyzer on Aeros-B," *J. Geophys.,* voL 40, pp. 585-592, 1974.

[8] W. C. Knudsen, K. Spenner, J. Bakke, and V. Novak, "Retarding potential analyzer for the Pioneer-Venus Orbiter mission," *Space Sci. Inst.,* vol. 4, pp. 351-372,1979.

[9] L. Colin and C. F. Hall, "The Pioneer-Venus program," *Space Sci. Rev.,* vol. 20, pp. 283-306, 1977

[10] L. Colin, "Encounter with Venus," *Science,* vol. 203, pp. 743745, 1979.

[11] W. C. Knudsen and K. K. Harris, "Ion-empact-produced secondary electron emission and its effect on space instrumentation," *J. Geophys. Res.,* vol. 78, pp. 1145-1152,1973.

[12] M. J. Drnyvesteyn, "Der Niedervoltbogen," Z. *Phys.,* vol. 64 pp. 781-798, 1930.

[13] W. C. Knudsen, K. Spenner, R. C. Whitten, J. R. Spreiter, K. L. Miller, and V. Novak, "Thermal structure and major ion composition of the Venus ionosphere: First RPA results from Venus orbiter," *Science,* vol. 203, pp. 757-763 1979.

[14] —, "Thermal structure and energy influx to the day and nightside Venus ionosphere," *Science,* vol. 205, pp. 105-107, 1979

[15] W. C. Knudsen, K. L. MiUer, K. Spenner, R. C. Whitten, and J R. Spreiter, "ion drift velocity measurements in the Venusian ionosphere," in *Abstract, EOS,* vol. 60, p. 303, 1979

[16] K. Spenner, W. C. Knudsen, K. L. MiUer, and V. Novak, "Observations of the Venus ionospheric mantle formed between ionosphere and ionosheath," in *Abstract, XVIIth General Assembly of the Int. Union Geodesy and Geophysics* (Canberra, Australia), Dec. 3, 1979.

Manuscript received September 1, 1979. The work of W. C. Knudsen and J. Bakke was supported by NASA under Contract NAS2-8811. The work of K. Spenner and V. Novak was supported by the Bundesmmister fur Forschung und Technologie under Contract Do238 (RV-B 28/73).

W. C. Knudsen and J. Bakke are with the Lockheed Palo Alto Research Laboratory, Palo Alto, CA 94304.

K. Spenner and V. Novak are with the Fraunhofer Institute fur Physikalische Weltraumforschung, 78 Freiburg, Federal Republic of Germany.

0196-2892/80/0100-0054$00.75

Fig 1 Assembled orbiter RPA.

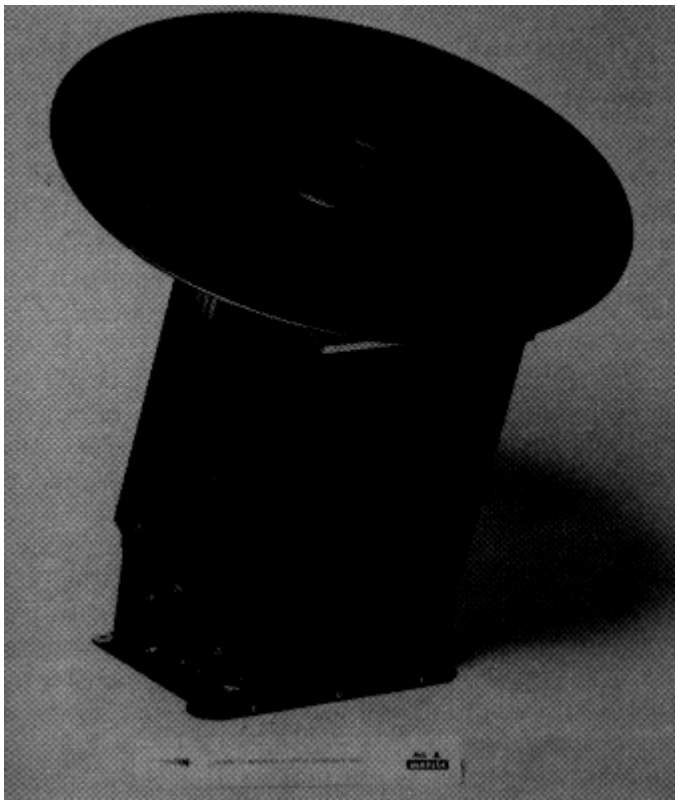

Fig 2. RPA integrated on the orbiter spacecraft.

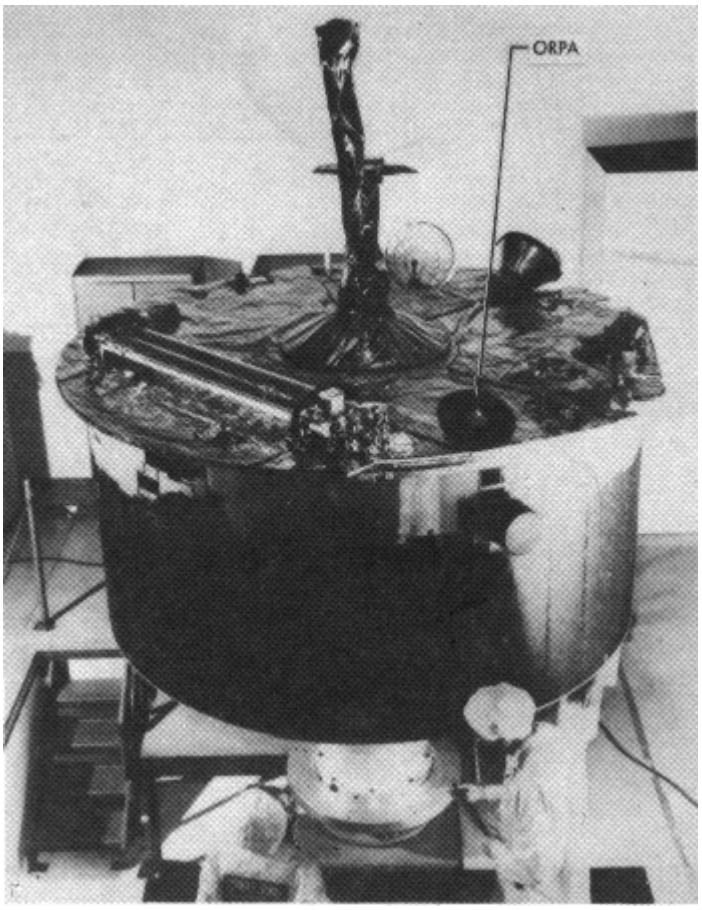

Fig 3. Schematic grid arrangement.

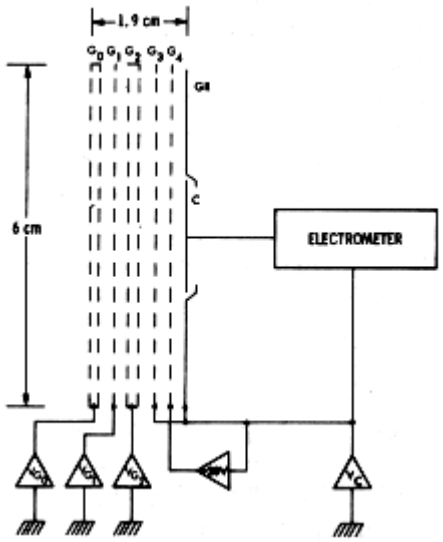

Fig 4. Electron characteristic curve telemetered in the *I-V* option and values of $\Delta\log(-I\varepsilon)$ selected by instrument logic and telemetered in the peak option. SZA is solar zenith angle.

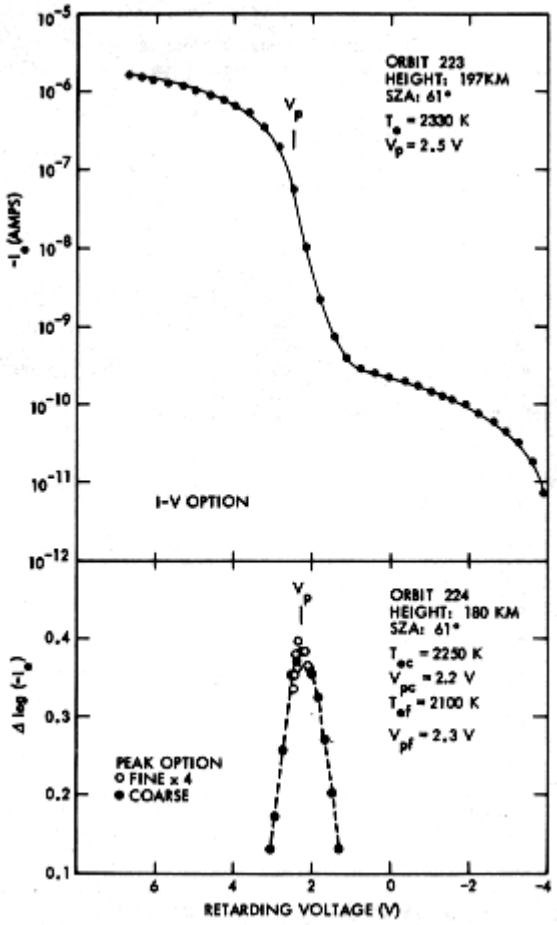

Fig 5. Ion characteristic curve telemetered in the *I-V* option and Δ*I* values selected by instrument logic in the peak option.

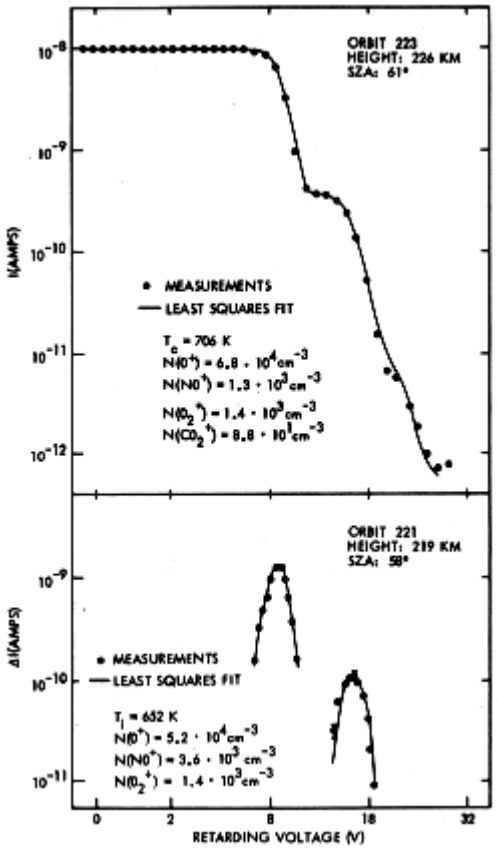

Fig 6. Measurment of ion-drift velocity by measuring a single drift velocity component in three independant directions in three successive spin periods.

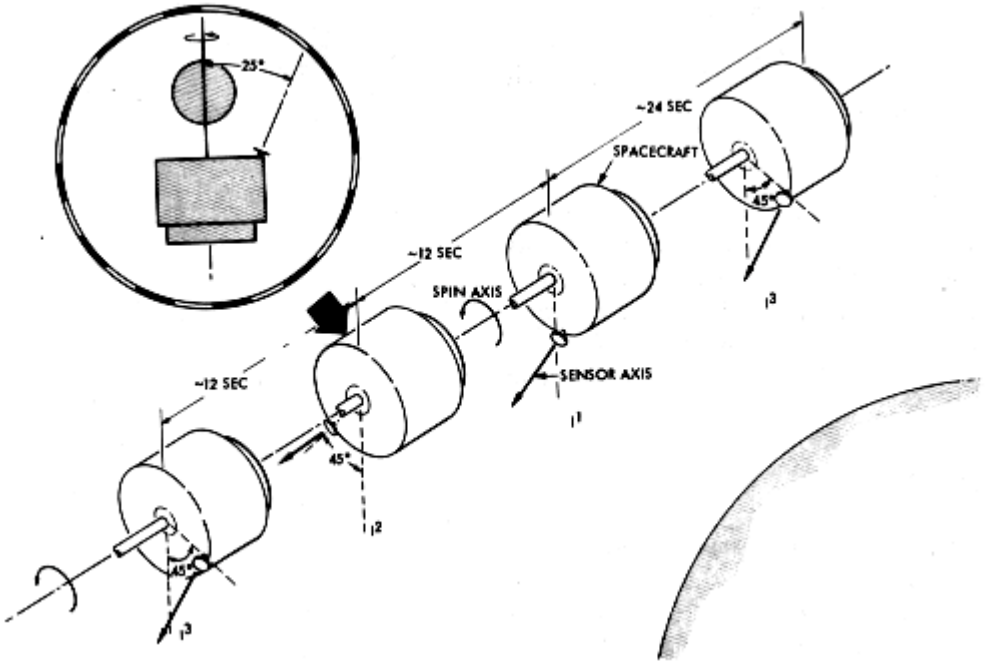

Fig 7. Electron current characteristics measured in the suprathermal-electron mode.

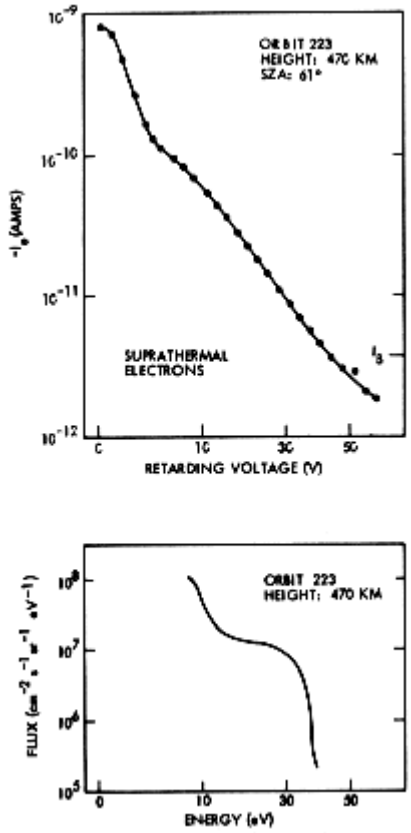

Table 1

TABLE I
MEASURED PLASMA QUANTITIES

Symbol	Quantity	Sample Distance[a] (km)	Closest Distance Between Samples[b] (km)	Range[c]	Uncertainty[d]
$N_i(=N_e)$	Total ion concentration	1×10^{-3}	20×10^{-3}	~10–$10^7\,cm^{-3}$	~5%
N_i^j	Concentrations of up to four abundant ions	1.6	120	$\sim10^2$–$10^7\,cm^{-3}$	~5%
T_i^j	Temperature of the jth ion	1.6	120	100–10,000 K $\sim10^2<N_i<10^7 cm^{-3}$	~5%
M_i^j	Mass of the jth ion	1.6	120	1–56 amu	~1 amu
$\bar{D}$	Ion drift velocity	1.6, 240	500	0.05–5 km s^{-1}	~50 m s^{-1}
fe	Low-energy electron distribution function	0.5	120	1–50 eV, $\sim10^6$–10^{12} $cm^{-2}s^{-1}sr^{-1}eV^{-1}$	~25%
T_e	Ionospheric electron temperature	0.4	0.4, 120	300–25,000K $\sim10^2\leq N_e\leq10^7 cm^{-3}$	~10%
T_e	Solar wind electron temperature	0.5	120	25,000–5×10^5K $N_e\geq0.5 cm^{-3}$	~25%
N_e	Solar wind electron concentration	0.5	120	~0.5–$10^2 cm^{-3}$	~30%

[a]This is the distance traveled by the spacecraft at a velocity of 10 km s^{-1} during which the plasma is sampled.
[b]This distance is dictated by assigned bit rate.
[c]These ranges depend in some instances on the values of other parameters such as ion composition.
[d]These uncertainties apply to the higher concentration ranges. As the concentration drops toward the lower range value, the accuracies will degrade.

Tables II and III

TABLE II
CONTROL VOLTAGE

Symbol	Element	Electron[a] Mode (V)	Ion[a] Mode (V)	Suprathermal[a] Electron Mode (V)
G_0	Entrance grid	6.8 to -4.2	0 or -4.6	0
G_1	Ion suppressor grid	6.8 to -4.2	-0.1[b] to 36[b]	47
G_2	Retarding grid	6.8 to -4.2	-0.1[b] to 36[b]	0 to -50
G_3	Displacement current shield	47	-4.6	47
G_4	Electron suppressor grid	27	-24.6	27
C, GR	Collector, guard ring	47	-4.6	47

[a]Referenced to satellite ground except where otherwise indicated.
[b]Referenced to plasma potential.

TABLE III
RETARDING POTENTIAL PROGRAMS

Mode	Scan	Number of Steps	Step Size (V)	Voltage Range[a] (V)
E	Electron, coarse	64	-0.176	6.8 to -4.6
	Electron, fine	20	-0.044[c]	0.88[c]
I	Ion	80	J x 0.011[d]	-0.1[b] to 36[b]
S	Suprathermal electron	48	J x 0.044[d]	0 to -50

[a]Referenced to satellite ground except where otherwise indicated.
[b]Referenced to plasma potential.
[c]Subdivides five coarse steps.
[d]The step size is proportional to step J.

Table 4

Instrument Parameter Summary

Parameter	Value
Current range (A)	$10^{-4} - 10^{-12}$
Current accuracy (percent)	98 (10 bit A/D)
Sampling interval (s)	0.002
Retarding voltage uncertainty (percent)	0.1
Bit rate (b/s)	40 or less
Commands	6
Power (W)	2.4
Weight (kg)	2.9
Volume (cm^3)	4440